Supplement of Hydrol. Earth Syst. Sci., 24, 1347–1366, 2020
https://doi.org/10.5194/hess-24-1347-2020-supplement

Hydrology and Earth System Sciences
Open Access

Supplement of

Dynamics of hydrological-model parameters: mechanisms, problems and solutions

Tian Lan et al.

Correspondence to: Kairong Lin (linkr@mail.sysu.edu.cn)

Contents of this file

Introduction

This supporting information includes five sections that support the analysis. The *1 SCE-UA algorithm* sections are used to support the *3.1 calibration schemes* section in the main manuscript. The *2 Violin plot* section is used to support the *5.2.1 A tool for convergence evaluation of dynamized parameters* section in the main manuscript. The *3 evaluation results of model performance in Mumahe basin and Xunhe basin* section is used to account for *4 results* section in the main manuscript. The *4 Convergence performance in Mumahe basin and Xunhe basin* section is used to supplement *5.2.2 Convergence assessment* section in the main manuscript.

S1 SCE-UA

The shuffled complex evolution approach (SCE-UA), as an effective global optimization method, is a commonly used algorithm, because it is open source and was the first algorithm aimed specifically at calibrating hydrological models (Khakbaz and Kazeminezhad, 2012;Eckhardt and Arnold, 2001;Duan et al., 1994;Sorooshian et al., 1993). The technical details about the SCE-UA can be shown in the flowchart (see Figure S1) (Duan et al., 1994). In the SCE-UA, the upper limit of the objective function evaluation is set to 10,000 times. All other settings of the SCE-UA technique are the default.

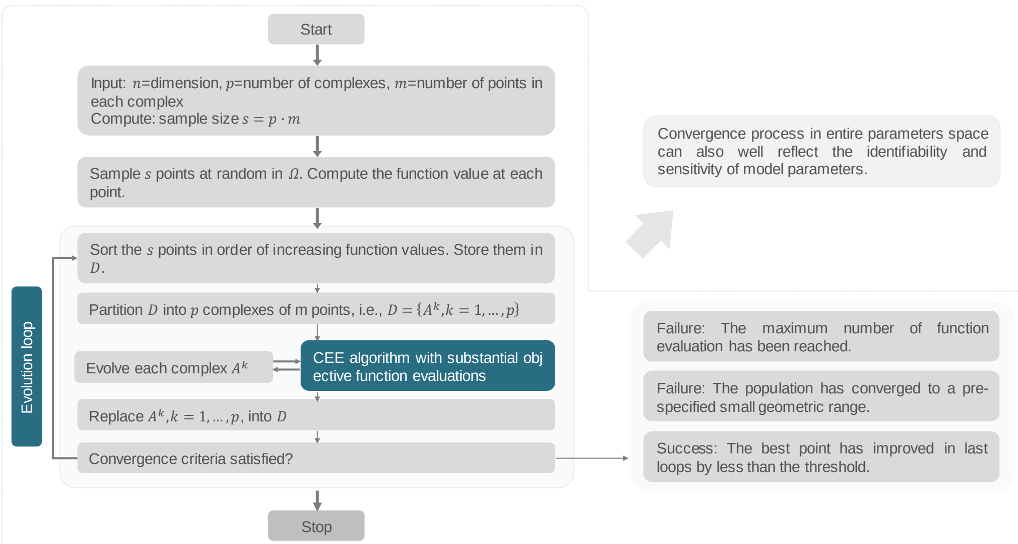

Figure S1. The flowchart of the SCE-UA algorithm (Duan et al., 1994; 1993; 1992).

S2 Violin plot

A violin plot is a combination of a Box Plot and a Density Plot showing more details of data distribution. As shown in Figure S2, the thick black bar in the center represents the interquartile range. The white dot represents the median. The thin black line is extended from the thick black bar and represents the 95% confidence intervals. On each side of the thin black line is a kernel density estimation to show the distribution shape of the data. Wider sections of the violin plot represent a higher probability that members of the population will take on the given value; the skinnier sections represent a lower probability (Hintze and Nelson, 1998). The violin plots can exactly show the kernel density distribution, avoiding the overlapping traditional density plot occur to become difficult to identify. Moreover, unlike bar graphs with means and error bars, violin plots contain all data points, which makes them an excellent tool to visualize samples of small sizes. Violin plots are perfectly appropriate even if your data do not conform to normal distribution. They work well to visualize both quantitative and qualitative data.

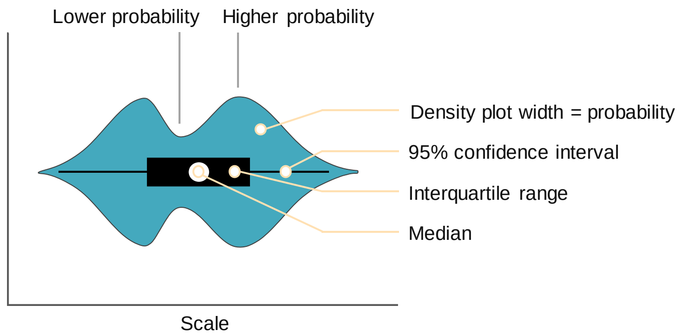

Figure S2. Anatomy of a violin plot

S3 Evaluation results of model performance in Mumahe basin and Xunhe basin

Table S1. Evaluation results of model performance for scheme 1 and scheme 5 in the Mumahe basin. The best performance is marked red.

	NSE	LNSE	RMSE_Q5	RMSE_Q20	RMSE_mid	RMSE_Q70	RMSE_Q95
				Calibration			
Scheme 1	0.691	0.445	0.953	0.357	0.118	0.554	0.909
Scheme 5	**0.324**	**0.262**	**0.362**	**0.070**	**0.112**	**0.288**	**0.729**
				Verification			
Scheme 1	0.750	0.686	1.082	0.342	0.183	0.825	1.450
Scheme 5	**0.345**	**0.325**	**0.338**	**0.056**	**0.165**	**0.524**	**0.717**
				Calibration-verification			
Scheme 1	0.059	0.241	0.129	-0.015	0.065	0.271	0.541
Scheme 5	**0.021**	**0.062**	**-0.023**	**-0.013**	**0.053**	**0.236**	**-0.013**

Table S2. The parameter sets of scheme 1 and scheme 5 in the Mumahe basin.

		H_{uz}	B	alpha	K_q	K_s
Scheme 1		916.692	1.990	0.048	1.000	0.079
Scheme 5	Dry period	999.540	1.990	0.051	0.501	0.038
	Rainfall period I	999.998	1.900	0.010	0.713	0.143
	Rainfall period II	27.799	1.990	0.010	0.801	0.237
	Rainfall period III	644.639	1.990	0.010	0.501	0.090

Minimum Maximum

Table S3. Evaluation results of model performance for scheme 1 and scheme 5 in the Xunhe basin. The best performance is marked red.

	NSE	LNSE	RMSE_Q5	RMSE_Q20	RMSE_mid	RMSE_Q70	RMSE_Q95

Calibration							
Scheme 1	0.617	0.334	0.495	0.164	0.304	0.192	0.573
Scheme 5	**0.252**	**0.183**	**0.165**	**0.153**	**0.157**	**0.166**	**0.724**
Verification							
Scheme 1	0.683	0.478	0.616	0.271	0.322	0.091	0.674
Scheme 5	**0.253**	**0.258**	**0.186**	**0.071**	**0.076**	**0.092**	**0.292**
Calibration-verification							
Scheme 1	0.066	0.144	0.120	0.107	0.018	**-0.100**	0.101
Scheme 5	**0.001**	**0.074**	**0.021**	**-0.055**	**-0.081**	-0.074	**-0.432**

Table S4. The parameter sets of scheme 1 and scheme 5 in the Xunhe basin. The best performance is marked red.

		H_{uz}	B	alpha	K_q	K_s
Scheme 1		999.991	1.259	0.342	0.894	0.024
Scheme 5	Dry period	999.943	0.391	0.565	0.506	0.011
	Rainfall period I	988.154	1.602	0.031	1.000	0.112
	Rainfall period II	353.777	0.641	0.010	0.500	0.319
	Rainfall period III	456.369	0.418	0.104	1.000	0.121

Minimum Maximum

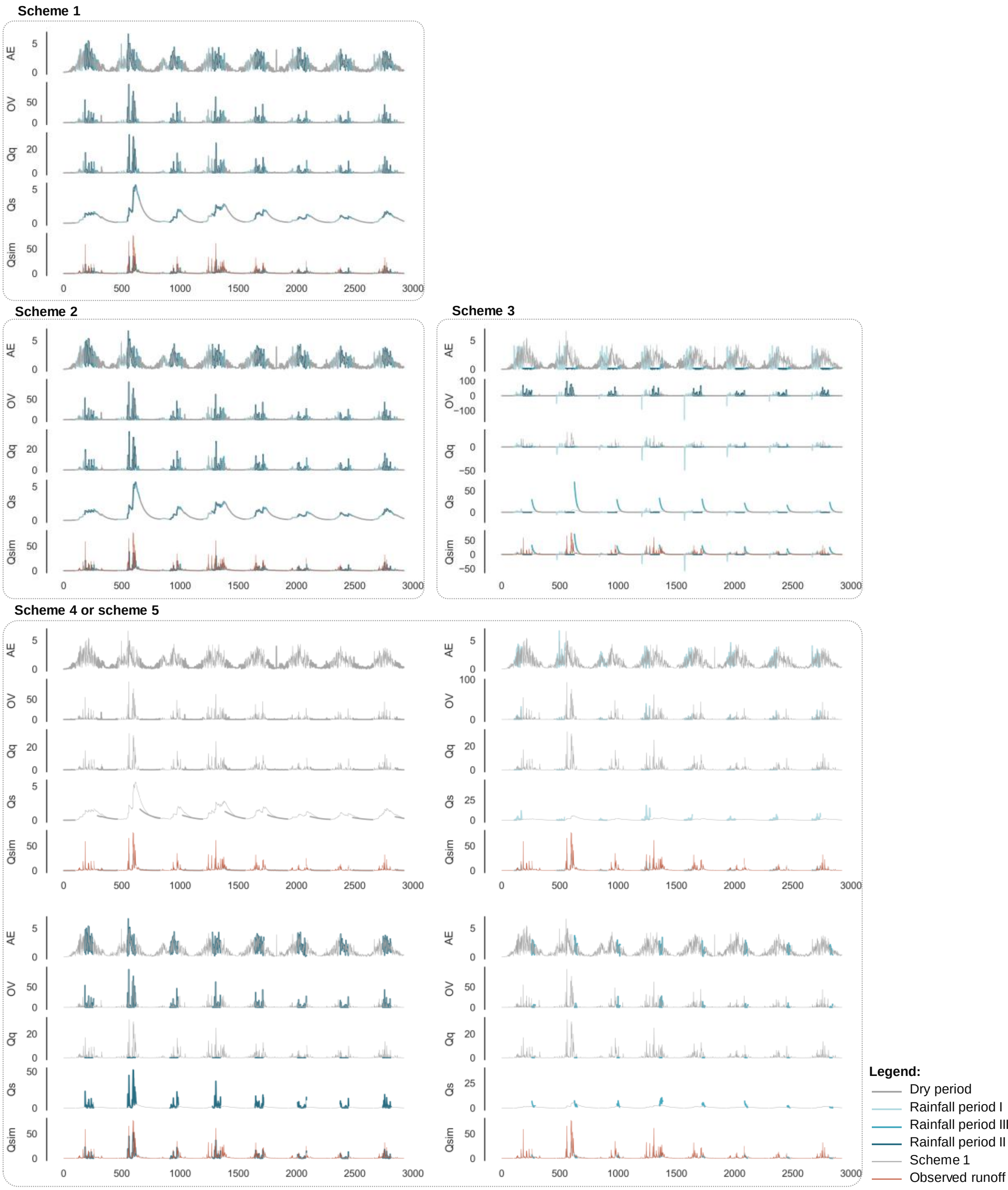

Figure S3. Fluxes assessment. All fluxes (including $\boldsymbol{AE}$, $\boldsymbol{OV}$, $\boldsymbol{Q_q}$, $\boldsymbol{Q_s}$, and $\boldsymbol{Q_{sim}}$) for five schemes in the whole calibration period in Hanzhong basin.

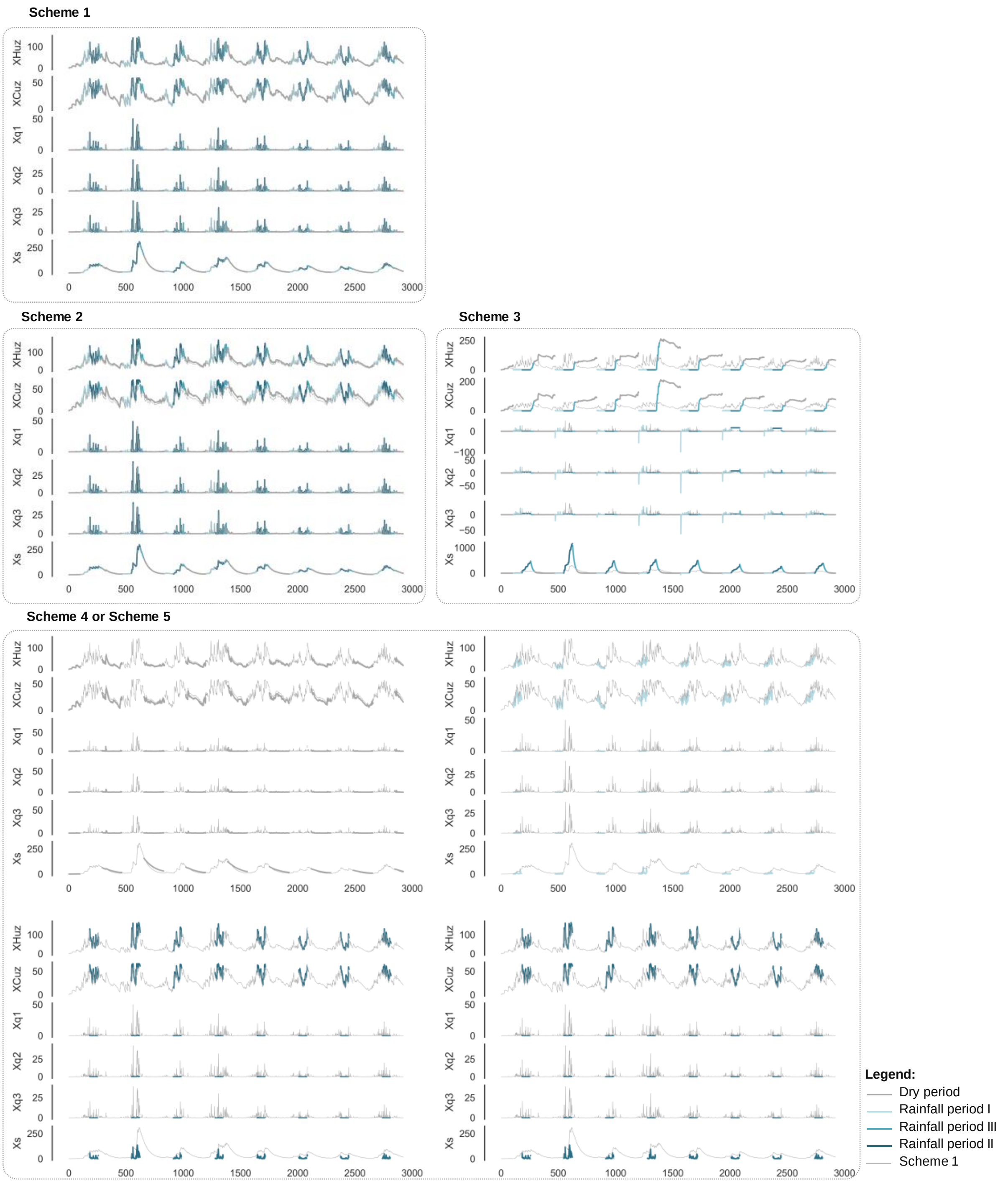

Figure S4. State variables assessment. All state variables (including XH_{UZ} XC_{UZ} X_{q1}, X_{q2}, X_{q3}, and X_s) for five schemes in the whole calibration period in Hanzhong basin.

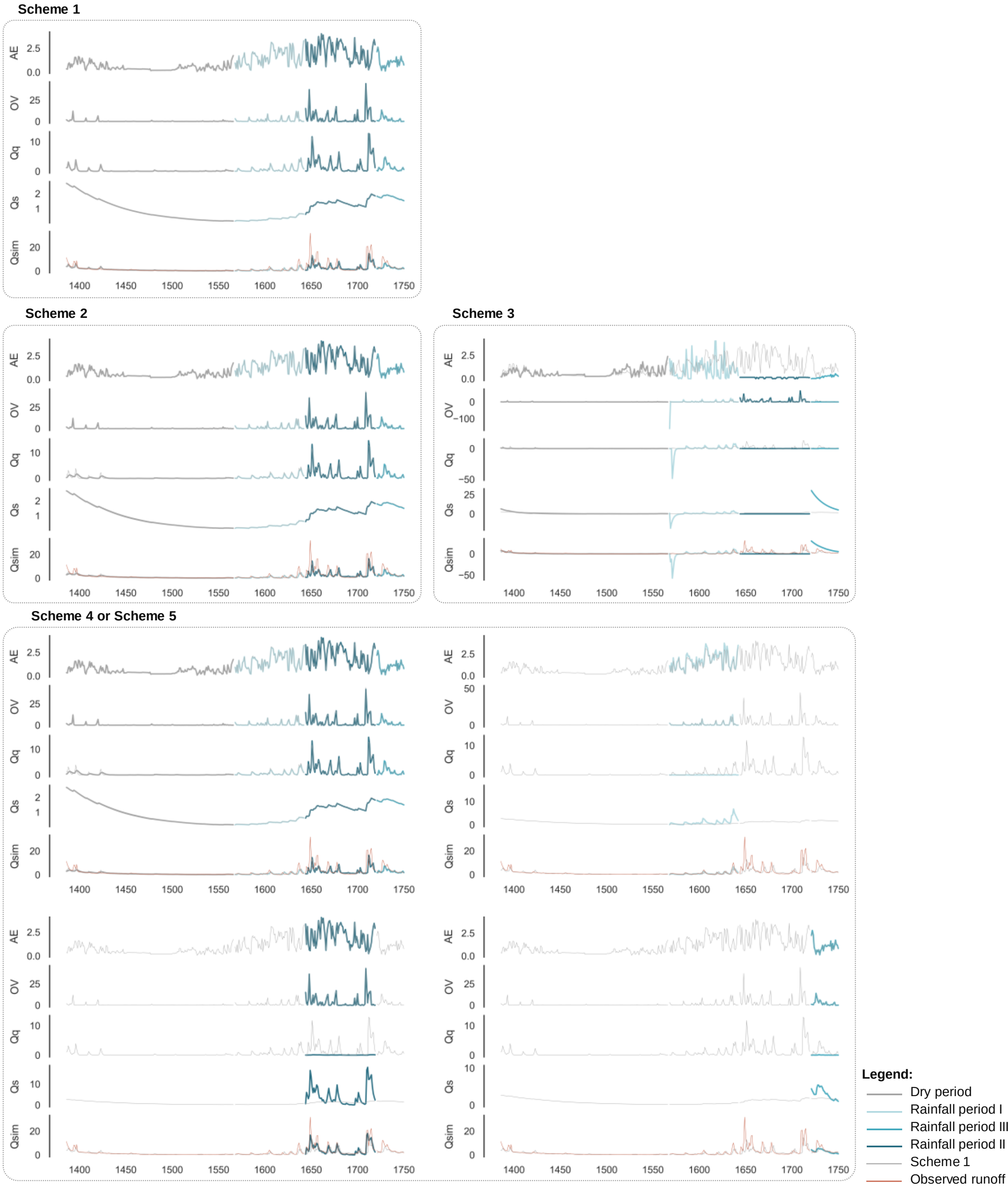

Figure S5. Fluxes assessment. All fluxes (including $\boldsymbol{AE}$, $\boldsymbol{OV}$, $\boldsymbol{Q_q}$, $\boldsymbol{Q_s}$, and $\boldsymbol{Q_{sim}}$) for five schemes in the calibration period in Hanzhong basin.

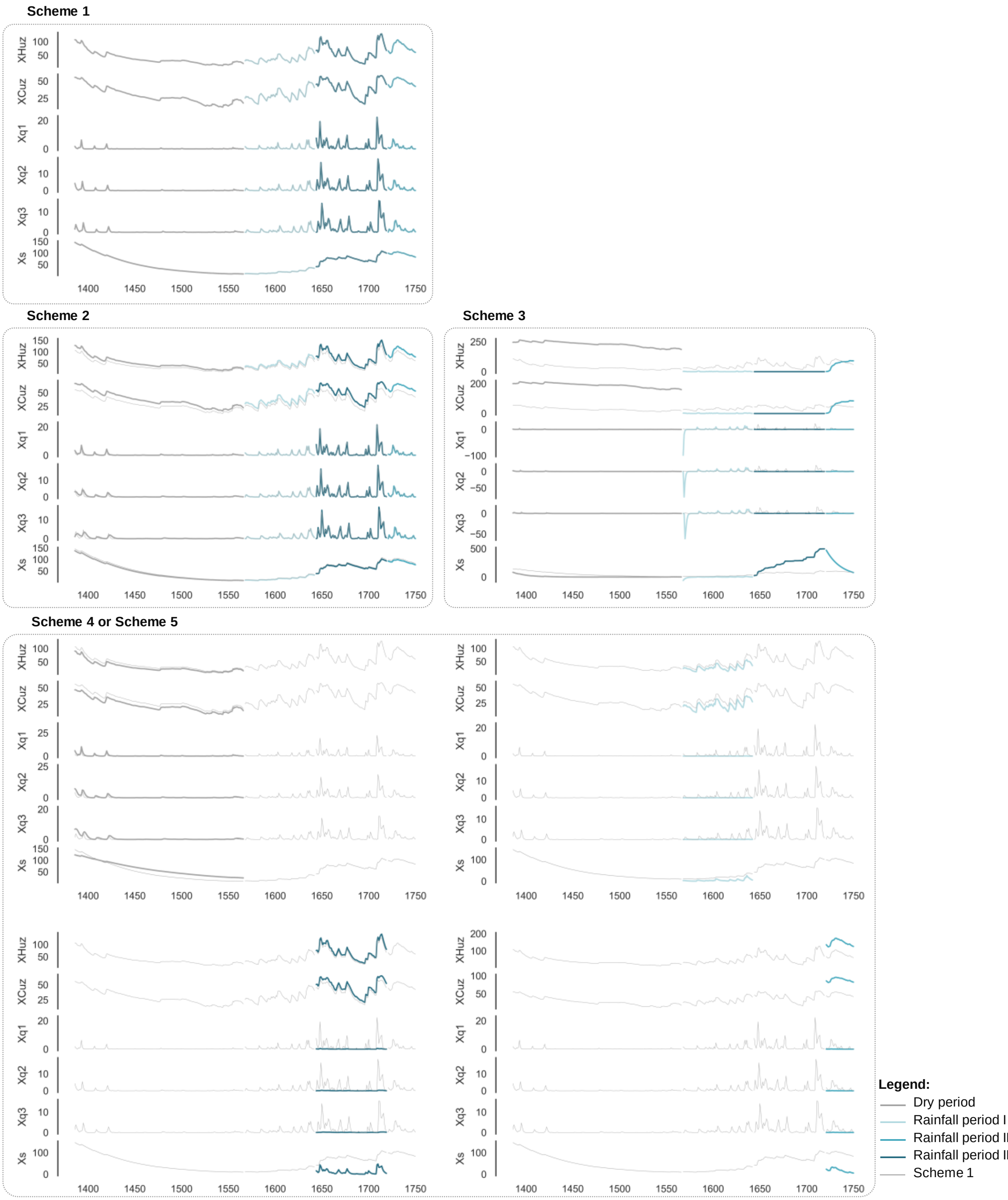

Figure S6. State variables assessment. All state variables (including XH_{UZ} XC_{UZ} X_{q1}, X_{q2}, X_{q3}, and X_s) for five schemes in the calibration period in Hanzhong basin.

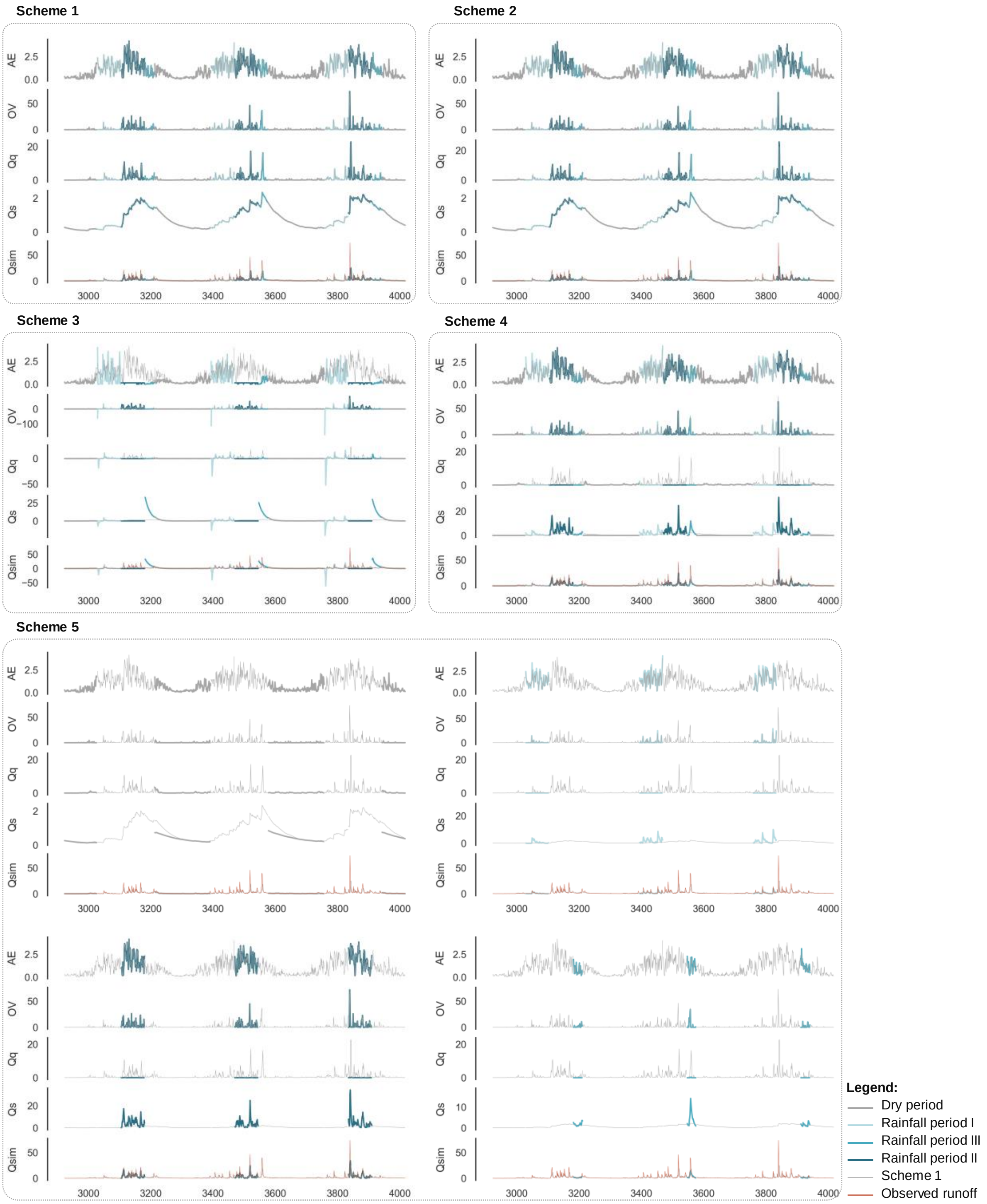

Figure S7. Fluxes assessment. All fluxes (including $\boldsymbol{AE}$, $\boldsymbol{OV}$, $\boldsymbol{Q_q}$, $\boldsymbol{Q_s}$, and $\boldsymbol{Q_{sim}}$) for five schemes in the whole verification period in Hanzhong basin.

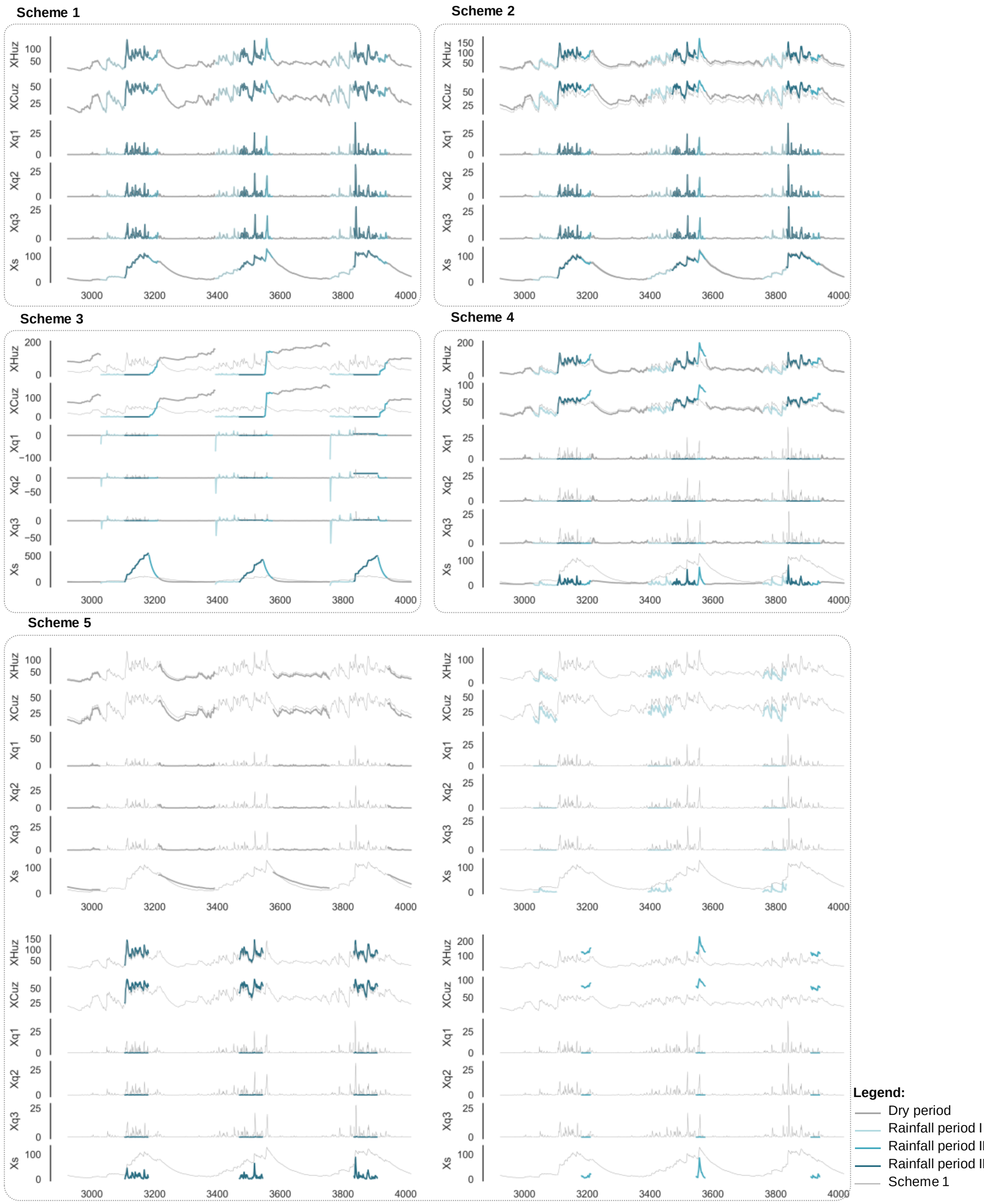

Figure S8. State variables assessment. All state variables (including XH_{UZ} XC_{UZ} X_{q1}, X_{q2}, X_{q3}, and X_s) for five schemes in the whole verification period in Hanzhong basin.

4 Convergence assessment in Mumahe basin and Xunhe basin

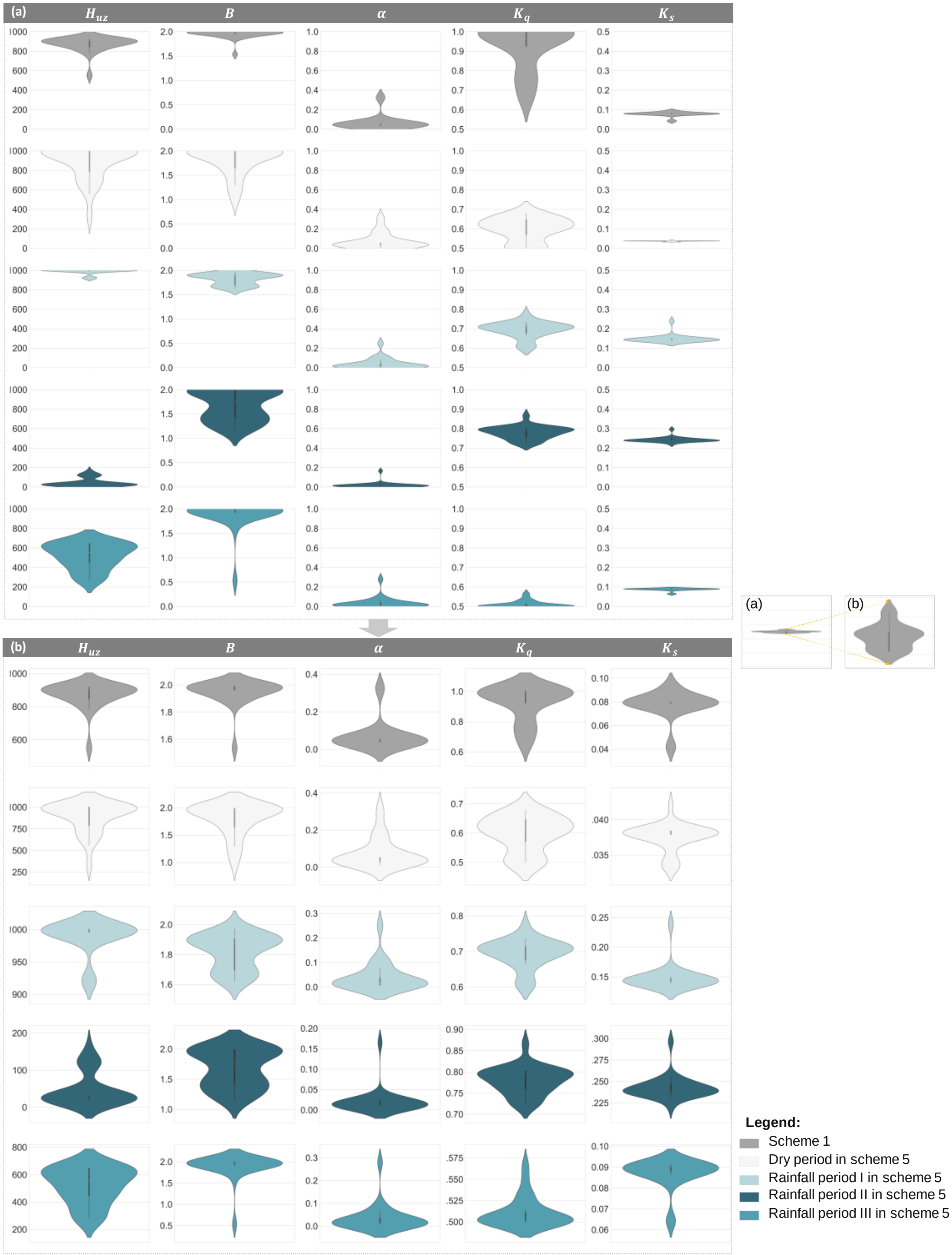

Figure S9. Convergence assessment. Convergence performance for scheme 1 and scheme 5 in Mumahe basin.

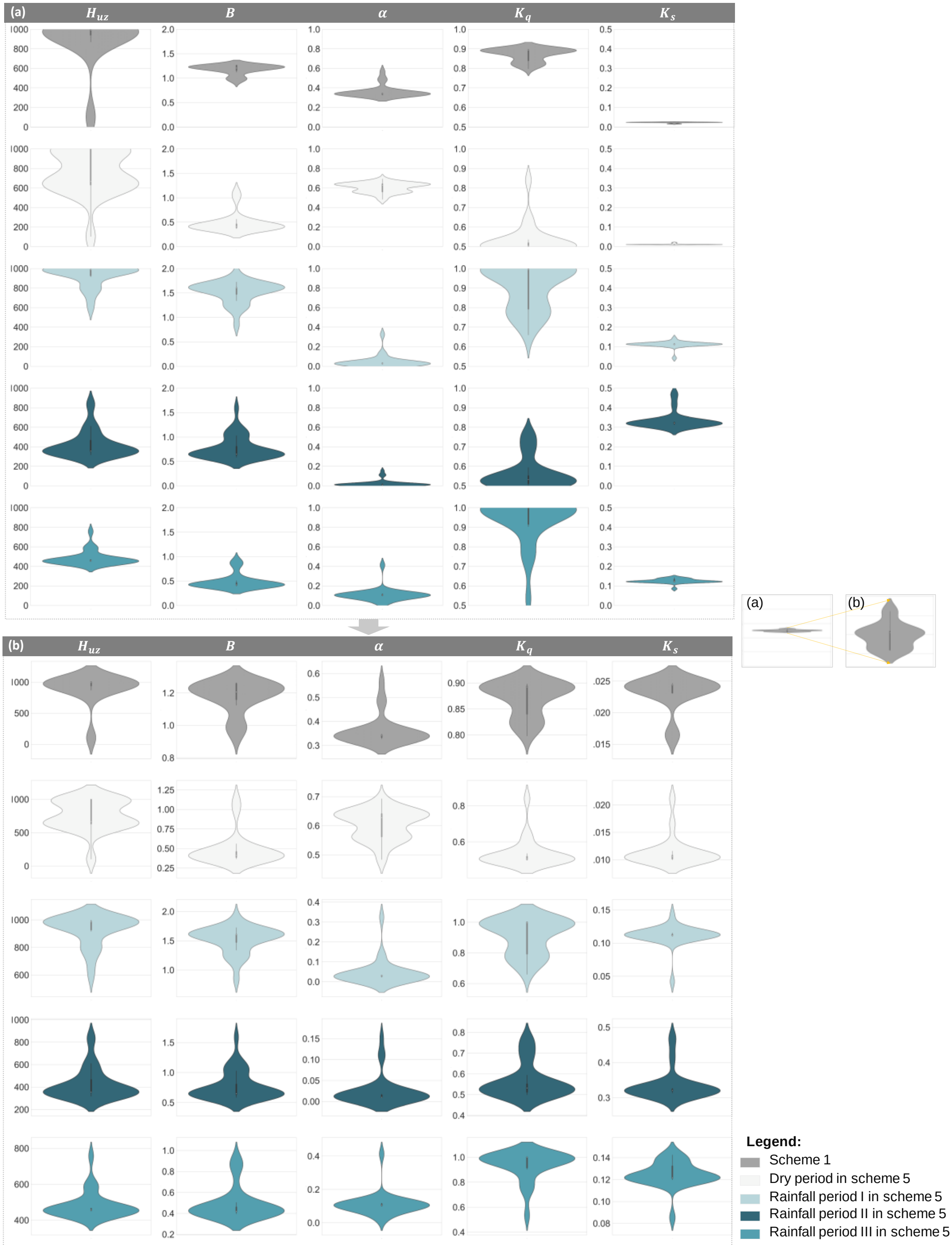

Figure S10. Convergence assessment. Convergence performance for scheme 1 and scheme 5 in Xunhe basin.

References

Chen, K. L., Mei, J. J., Rehren, T., and Zhao, C. C.: Indigenous production and interregional exchange: late second-millennium BC bronzes from the Hanzhong basin, China, Antiquity, 90, 665-678, https://doi.org/10.15184/aqy.2016.94, 2016.

Cheng, L., Yaeger, M., Viglione, A., Coopersmith, E., Ye, S., and Sivapalan, M.: Exploring the physical controls of regional patterns of flow duration curves – Part 1: Insights from statistical analyses, Hydrol Earth Syst Sc, 16, 4435-4446, 10.5194/hess-16-4435-2012, 2012.

Coopersmith, E., Yaeger, M. A., Ye, S., Cheng, L., and Sivapalan, M.: Exploring the physical controls of regional patterns of flow duration curves – Part 3: A catchment classification system based on regime curve indicators, Hydrol Earth Syst Sc, 16, 4467-4482, 10.5194/hess-16-4467-2012, 2012.

Duan, Q. Y., Gupta, V. K., and Sorooshian, S.: Shuffled complex evolution approach for effective and efficient global minimization, Journal of Optimization Theory and Applications, 76, 501-521, 10.1007/bf00939380, 1993.

Duan, Q. Y., Sorooshian, S., and Gupta, V. K.: Optimal use of the SCE-UA global optimization method for calibrating watershed models, J. Hydrol., 158, 265-284, https://doi.org/10.1016/0022-1694(94)90057-4 1994.

Duan, Q., Sorooshian, S., and Gupta, V.: Effective and efficient global optimization for conceptual rainfall-runoff models, Water Resources Research, 28, 1015-1031, 10.1029/91WR02985, 1992.

Eckhardt, K., and Arnold, J. G.: Automatic calibration of a distributed catchment model, Journal of Hydrology, 251, 103-109, https://doi.org/10.1016/s0022-1694(01)00429-2, 2001.

Fang, J., Song, Y., Liu, H., and Piao, S.: Vegetation-climate relationship and its application in the division of vegetation zone in China, Acta Botanica Sinica, 44, 1105-1122, 2002.

Hintze, J. L., and Nelson, R. D.: Violin plots: a box plot-density trace synergism, The American Statistician, 52, 181-184, https://doi.org/10.2307/2685478, 1998.

Khakbaz, F., and Kazeminezhad, M.: Work hardening and mechanical properties of severely deformed AA3003 by constrained groove pressing, Journal of Manufacturing Processes, 14, 20-25, https://doi.org/10.1016/j.jmapro.2011.07.001, 2012.

Kim, D., and Kaluarachchi, J.: Predicting streamflows in snowmelt-driven watersheds using the flow duration curve method, Hydrol Earth Syst Sc, 18, 1679-1693, 10.5194/hess-18-1679-2014, 2014.

Li, Z. J., Liu, P., Deng, C., Guo, S. L., He, P., and Wang, C. J.: Evaluation of Estimation of Distribution Algorithm to Calibrate Computationally Intensive Hydrologic Model, J Hydrol Eng, 21, 04016012, https://doi.org/10.1061/(asce)he.1943-5584.0001350, 2016.

Lin, K. R., Zhang, Q., and Chen, X. H.: An evaluation of impacts of DEM resolution and parameter correlation on TOPMODEL modeling uncertainty, J. Hydrol., 394, 370-383, https://doi.org/10.1016/j.jhydrol.2010.09.012, 2010.

Pfannerstill, M., Guse, B., and Fohrer, N.: Smart low flow signature metrics for an improved overall performance evaluation of hydrological models, Journal of Hydrology, 510, 447-458, https://doi.org/10.1016/j.jhydrol.2013.12.044, 2014.

Pugliese, A., Castellarin, A., and Brath, A.: Geostatistical prediction of flow–duration curves in an index-flow framework, Hydrol Earth Syst Sc, 18, 3801-3816, 10.5194/hess-18-3801-2014, 2014.

Sorooshian, S., Duan, Q., and Gupta, V. K.: Calibration of rainfall-runoff models: Application of global optimization to the Sacramento Soil Moisture Accounting Model, Water Resour. Res., 29, 1185–1194, https://doi.org/10.1029/92wr02617, 1993.

Sun, X., Lu, H., Wang, S., and Yi, S.: Ages of Liangshan Paleolithic sites in Hanzhong Basin, central China, Quat Geochronol, 10, 380-386, https://doi.org/10.1016/j.quageo.2012.04.014, 2012.